Computer Assisted Mechanics and Engineering Sciences, **17**: 99–112, 2010.

Method of fundamental solutions and random numbers for the torsion of bars with multiply connected cross sections

Piotr Gorzelańczyk
Higher Vocational State School Pila, Polytechnic Institute
Podchorążych 10, 64-920 Piła, Poland
e-mail: piotr.gorzelanczyk@pwsz.pila.pl

The torsion of bars with multiply connected cross section by means of the method of fundamental solutions (MFS) is considered. Random numbers were used to determine the minimal errors for MFS. Five cases of cross sections are examined. The numerical results for different cross sectional shapes are presented to demonstrate the efficiency and accuracy of the method. Non-dimensional torsional stiffness was calculated by means of numerical integration of stress function for one of the cases. This stiffness was compared with the exact stiffness for the first case and with the stiffness resulting from Bredt's formulae for thin-walled cross sections.

Keywords: Bredt's formulae, method of fundamental solutions, multiply connected sections, random numbers.

1. Introduction

The solution of the torsion problem for multiply connected cross section is more difficult than for the simply connected one. Probably this is the reason why there are not too many papers considering this problem. For a doubly connected cross section, the exact solution exists for the annular cross section. Weinel [1] proposed the solution for a doubly connected cross section with eccentric circles. In the work [2], it was found that for the doubly connected domains with a prescribed area of the hole and the cross section, the ring bounded by two concentric circles has the maximal torsional rigidity. The authors in the book [3] present the description of the method of solution of the torsion problem for doubly connected cross section in which outer and inner contours are rectangles. This method was proposed by Russian authors in a series of papers in the 1950s and it is based on expansion of stress function into a Fourier series. In order to obtain an effective solution, this method requires the solution of infinite system of linear equations. Wang [4] presented a method for torsion analysis of two connected cross sections in a shape of flattened tube consisting of two half-annular pieces and two rectangular pieces. It adopted an approximate solution in the form of truncated series of functions of its own. In addition, to satisfy the boundary conditions, it used the boundary element methods. In the work [5], Wang generalized this method to treat two arbitrary connected cross sections consisting of circular arcs and straight lines, all with a uniform thickness. A modified Fourier series method for the torsion analysis of bars with multiply connected cross sections was presented in the work [6]. The effectiveness of this method was presented for polygonal cross sections with polygonal holes.

Mejak [7] presented a method for an optimal shape design of doubly connected bars in torsion. He solved the problem numerically by the finite element method. In the work [8], the Trefftz method, using special-purpose T-functions, was utilized to solve the problem of torsion. As examples, the singly connected, multiply connected and composite cross sections of bars in the shape of regular polygons were considered. The proposed Trefftz function not only satisfies governing equation but also the boundary conditions on some sides. In the article, the boundary collocation methods and the method of the last squares were used for the stress function. Using the analytical integration, an analytical solution for the dimensionless stiffness of the bar was obtained.

A special group of papers considers the thin-walled cross sections. A simple formulation for the torsion analysis of the thin-walled, hollow bars, which was proposed by Bredt [9], can be found in elementary textbooks of strength of materials. In the work [10], the author proves that Bredt's theory remains truer for thin tubes with multicell cross sections than for doubly connected. A closed-form expression for the torsion constant and the thin-walled typical multicell profiles is presented in the work [11]. Generalization of Bredt's method for moderately thick and hollow tubes with polygonal shapes is given in the work [12]. The purpose of this paper is the application of the Method of Fundamental Solutions and random numbers to torsion problem with multiply connected cross sections.

This method belongs to the so-called meshless methods which have been more and more popular in last two decades. The MFS was first proposed by the Georgian researchers Kupradze and Aleksidze [13]. Its numerical implementation was carried out by Mathon and Johnston [14]. The mathematical analysis (convergence and stability) of this method was considered in papers [15–20]. The comprehensive reviews of the MFS for various applications can be found in [21–22]. However, the method of fundamental solutions has been applied basically for simply connected regions. There are only few papers with the application of MFS for annular region, e.g., [23–25].

This paper presents the application of this method to multiply connected cross sections, namely: (I) circular with circular centered hole, (II) square with circular centered hole, (III) square with square centered hole, (IV) circular with two circular symmetrically placed holes, (V) square with two circular symmetrically placed holes.

In this paper, searching for solutions was used to determine minimal errors of the method of fundamental solutions. In the first step, the error on the inner and outer contour was determined for the set of variable coefficients. Next, its minimum value was determined. This method turned out to be a very time-consuming task, because it required a lot of errors to be searched. Therefore to reduce this very large number of searched errors, random numbers were used. So far, no authors have used random numbers to determine the minimum errors of MRP.

2. Formulation of the problem

The problem of torsion of prismatic bars with multiply connected cross section (see Fig. 1) is formulated in terms of stress function, which satisfies Poisson's equation [26]:

$$\nabla^2\psi = -2\mu\omega \quad \text{in} \quad \Omega, \tag{1}$$

with boundary condition on the outer contour:

$$\psi = 0 \quad \text{on} \quad \Gamma_0, \tag{2}$$

and boundary conditions on the inner contour:

$$\psi = \psi_i \quad \text{on} \quad \Gamma_i, \qquad i = 1, 2, \ldots, n, \tag{3}$$

where $\psi(x, y)$ is stress function, μ is shear modulus of bar material, ω is angle of twist of bar per unit length, ψ_i are unknown values of constant of stress function at inner contours, n – number of hollow areas.

For determination of unknown constants ψ_i the following integral relations (Bredt's theorem) are given:

$$\oint_{\Gamma_i} \frac{\partial\psi}{\partial n} ds = -2\Omega_i\mu\omega, \qquad i = 1, 2, \ldots, n, \tag{4}$$

where Ω_i is area bounded by Γ_i.

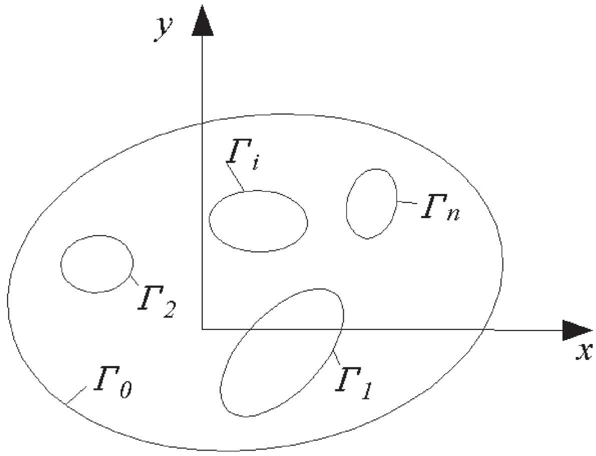

Fig. 1. Multiply connected cross sections of bar.

After introducing the non-dimensional variables:

$$X = \frac{x}{a}, \qquad Y = \frac{y}{a}, \qquad \Psi(X,Y) = \frac{\psi(x,y)}{a^2\mu\omega}. \tag{5}$$

The considered boundary value problem has the following dimensionless form governing equation for stress function:

$$\frac{\partial^2\Psi}{\partial X^2} + \frac{\partial^2\Psi}{\partial Y^2} = -2 \text{ in } \widetilde{\Omega}, \tag{6}$$

with boundary condition at outside contour:

$$\Psi = 0 \text{ on } \widetilde{\Gamma}_0 \tag{7}$$

and boundary condition at inner contour:

$$\Psi = \Psi_i \text{ on } \widetilde{\Gamma}_i, \qquad i = 1, 2, \ldots, n \tag{8}$$

and integral relation in the form:

$$\oint_{\widetilde{\Gamma}_i} \frac{\partial\Psi}{\partial n} ds = -2 \cdot \widetilde{\Omega}_i, \qquad i = 1, 2, \ldots, n, \tag{9}$$

where $\widetilde{\Omega}_i$ is dimensionless area bounded by $\widetilde{\Gamma}_i$.

3. Method of solution

In the MFS, the approximate solution of the problem is represented in the form of a linear superposition of source functions (fundamental solutions) with singular points that are located outside the domain of the problem. These points, called source points, are located on a "pseudo-boundary" outside the region. The "pseudo-boundary" has no common points with the boundary of the region. Because the fundamental solution satisfies the differential equation at any point, except at the source point; it follows that this representation satisfies exactly the governing equation, whereas the boundary conditions are only satisfied approximately. Therefore, the MFS belongs to the group of Trefftz methods for which it is essential that the governing equation is exactly satisfied. The weights of coefficients, which occur in the approximate solution, are determined by the satisfaction of the boundary condition, usually on a set of boundary points (collocation points). Using MFS, the solution of boundary value problem formulated by (6–9) can now be given as the sum of the particular solution and the homogeneous solution:

$$\Psi = -\frac{1}{2}\left(X^2+Y^2\right) + \sum_{j=1}^{MO} c_j \ln\left[(X-XSO_j)^2 + (Y-YSO_j)^2\right] + \sum_{i=1}^{n}\sum_{k=1}^{WIi} c_k^{(i)} \ln\left[\left(X-XSI_k^{(i)}\right)^2 + \left(Y-YSI_k^{(i)}\right)^2\right], \tag{10}$$

where XSO_j, YSO_j are coordinates of source points which are placed outside the region $\widetilde{\Omega}$ (Fig. 2), $XSI_k^{(i)}$, $YSI_k^{(i)}$ are coordinates of source points which are placed inside of inner contours $\widetilde{\Gamma}_i$, where $i = 1,2,\ldots,n$, MO is the number of source points outside the region $\widetilde{\Omega}$, MIi is the number of source points inside each inner contours $\widetilde{\Gamma}_i$, c_j and $c_k^{(i)}$ are unknown coefficients.

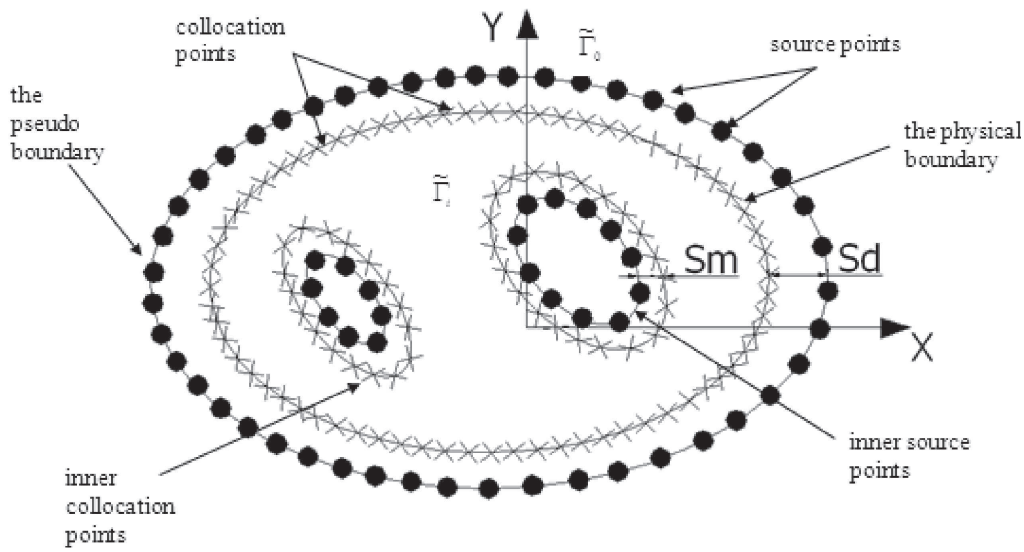

Fig. 2. Arrangement of the source points on the similar contour.

The unknown coefficients c_j, $c_k^{(i)}$ and constants Ψ_i are determined by collocation of boundary conditions (7, 8) and application of the integral relations (9).

In order to do this, NCO collocation points on outer contour with coordinates XCO_l, YCO_l as well as NCI collocation points on each inner contour with coordinates $XCI_m^{(i)}$, $YCI_m^{(i)}$ are chosen.

Substituting solution (10) into the boundary condition (7) we obtain:

$$\sum_{j=1}^{MO} c_j \ln\left[(XCO_l-XSO_j)^2 + (YCO_l-YSO_j)^2\right] + \sum_{i=1}^{n}\sum_{k=1}^{MIi} c_k^{(i)} \ln\left[(XCO_l-XSI_k^{(i)})^2 + (YCO_l-YSI_k^{(i)})^2\right] = \frac{1}{2}(XCO_l^2+YCO_l^2), \qquad l = 1,2,\ldots,NCO. \tag{11}$$

Similarly, substitution of solutions (10) into boundary condition (8) leads to a system of linear equations:

$$\sum_{j=1}^{MO} c_j \ln\Big[(XCI_m^{(i)} + XSO_j)^2 + (YCI_m^{(i)} - YSO_j)^2\Big] + \sum_{i=1}^{n}\sum_{k=1}^{MIi} c_k^{(i)} \ln\Big[(XCI_m - XSI_k^{(i)})^2 + (YCI_m - YSI_k^{(i)})^2\Big] = \frac{1}{2}(XCO_l^2 + YCO_l^2) + \Psi_i, \qquad m = 1,2,\ldots,NCI. \tag{12}$$

Using Bredt's conditions (9) on the inner contour $\widetilde{\Gamma}_i$ we have:

$$\sum_{j=1}^{MO} c_j \oint_{\widetilde{\Gamma}_i} \frac{\partial}{\partial n} \ln\Big[(X_s + XSO_j)^2 + (Y_s - YSO_j)^2\Big] ds + \sum_{i=1}^{n}\sum_{k=1}^{MIi} c_k^{(i)} \oint_{\widetilde{\Gamma}_i} \frac{\partial}{\partial n} \ln\Big[\Big(X_s - XSI_k^{(i)}\Big)^2 + \Big(Y_s - YSI_k^{(i)}\Big)^2\Big] ds = 0, \tag{13}$$

for $i = 1,2,\ldots,n$.

In this way we obtain $NCO + n \cdot NCI + n$ equations with $MO + n \cdot MIi + n$ unknowns.

For further numerical calculations the following assumptions: $M = MO + MIi$ and $NC = NCO + NCI$ were adopted.

4. Torsional stiffness and stress

The relations between the nonzero components of stress and stress function are given by following formulae:

$$\tau_{yz} = -\frac{\partial\psi}{\partial x}, \qquad \tau_{xz} = \frac{\partial\psi}{\partial y}. \tag{14}$$

The torsional moment is given by integral of the shear stresses over the area, which gives:

$$SZ = \iint (\tau_{yz}x - \tau_{xz}y)\,dxdy = -\iint \frac{\partial\psi}{\partial x} xdxdy - \iint \frac{\partial\psi}{\partial y} ydxdy + 2\sum_{i=1}^{n} \Omega_i\psi_i. \tag{15}$$

After simple manipulation, we get:

$$SZ = 2\iint \psi dxdy + 2\sum_{i=1}^{n} \Omega_i\psi_i. \tag{16}$$

By introducing the non-dimensional variables into (16) the torsional moment can be related to non-dimensional stress function:

$$SZ = \mu \cdot \omega \cdot a^4 \cdot \left[2\iint \Psi(X,Y)dXdY + 2\sum_{i=1}^{n} \widetilde{\Omega}_i\Psi_i\right]. \tag{17}$$

Next, the non-dimensional torsional stiffness can by expressed as:

$$M_s = \frac{SZ}{\mu \cdot \omega \cdot a^4} = 2\iint \Psi(X,Y)dXdY + 2\sum_{i=1}^{n} \widetilde{\Omega}_i\Psi_i. \tag{18}$$

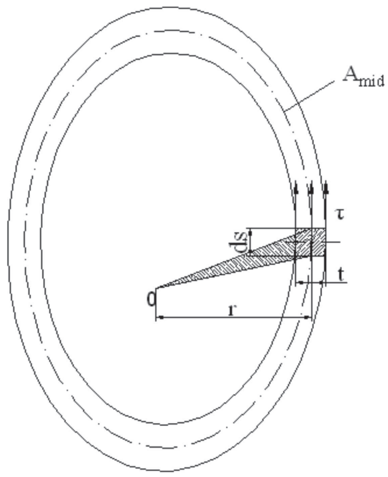

Fig. 3. Thin-walled bar with closed cross-section.

In the elementary textbooks about strength of materials [9] one can find the expression for torsion stiffness for the thin-walled hollow bars (Fig. 3), known as Bredt's formula:

$$SZ = \frac{4 \cdot \mu \cdot A_{\text{mid}}^2 \cdot \omega}{\oint \dfrac{ds}{t}}, \tag{19}$$

where A_{mid} is the area bounded by the centerline of the wall cross section, t is thickness.

5. Test examples

In order to demonstrate the accuracy and the effectiveness of the proposed method, seven cases of cross sections are considered: (I) circular with circular centered hole, (II) square with circular centered hole, (III) square with square centered hole, (IV) circular with two circular symmetrically placed holes and (V) square with two circular symmetrically placed holes.

The formulation of boundary values problems for seven considered cross sections in terms of non-dimensional stress function $\Psi(X, Y)$ is given in Figs. 4–8. In this problem, the thickness E is a parameter of structure which changes in a permissible range, i.e., $0 < E < 0.5$ for problems I-III and $0 < E < 0.25$ for problems IV and V.

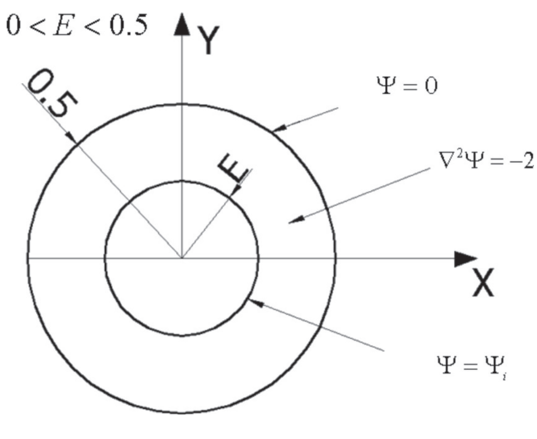

Fig. 4. Formulation of boundary value problem for circular with circular centered hole cross section of a bar. Problem I.

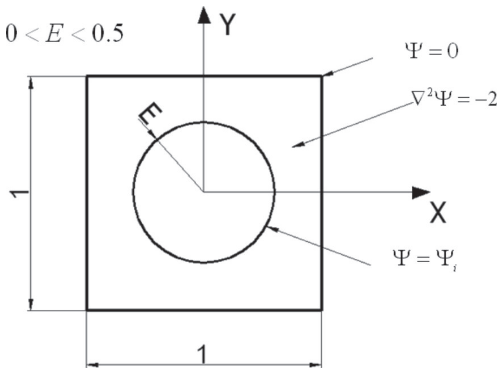

Fig. 5. Formulation of boundary value problem for square with circular centered hole cross section of a bar. Problem II.

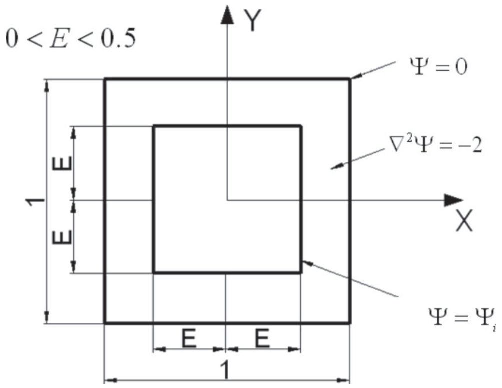

Fig. 6. Formulation of boundary value problem for square with square centered hole cross section of a bar. Problem III.

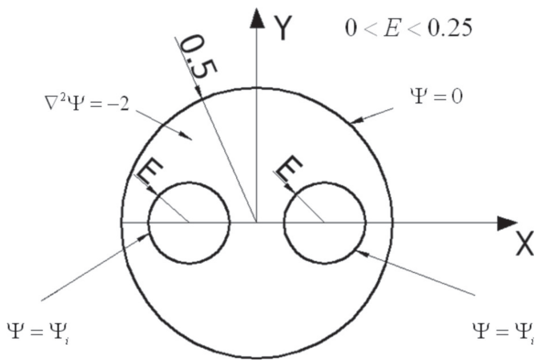

Fig. 7. Formulation of boundary value problem for circular with two circular symmetrically placed holes cross section of a bar. Problem IV.

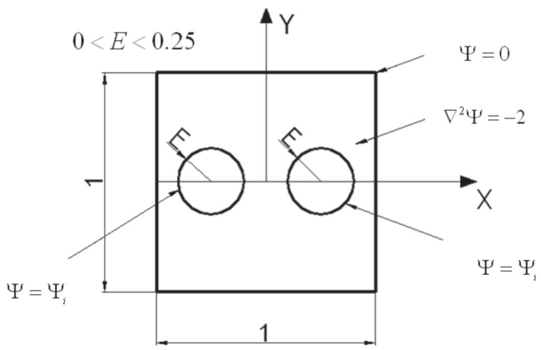

Fig. 8. Formulation of boundary value problem for square with two circular symmetrically placed holes section of a bar. Problem V.

On the basis of [27], the maximum relative error on the outer and inner boundary is determined as follows:

$$\delta_{MAXo} = \frac{\max |\Psi_{\text{outer}}|}{\max(i)\,|\Psi_{\text{mid}_{\text{outer\_}i}}|}, \tag{20}$$

$$\delta_{MAXin\_i} = \frac{\max |\Psi_{\text{outer\_}i} - \Psi_{\text{mid}_{\text{inner\_}i}}|}{\max(i)\,|\Psi_{\text{mid}_{\text{inner\_}i}}|}, \tag{21}$$

where δ_{MAXo} – is the maximal error on the outer contour, $\delta_{\text{MAXin\_}i}$ – is the maximal error on the inner contour, where $i = 1$ for the problems I-III and $i = 1, 2$ for the problems IV and V, Ψ_{outer} – is the value of the stress function on the outer contour, $\Psi_{\text{mid}_{\text{inner\_}i}}$ – is the middle value of the stress function on the inner contour, where $i = 1$ for the problems I-III and $i = 1, 2$ for the problems IV and V.

6. Numerical results

In this paper, the MFS applied to the problem of torsion of a prismatic bar depends on number of parameters. These parameters are as follows: the distance of the outer contour containing the source points from the boundary – Sd, the distance of the inner contour containing the source points from the boundary – Sm (Fig. 2), number of source points – NC, number of collocation points – M, and thickness of the elements – E. A minimum error was founded for different values of E in the paper. In this case, the error is multidimensional, with many local minima (Fig. 9). Figure 9 shows that the error function has many local minimums.

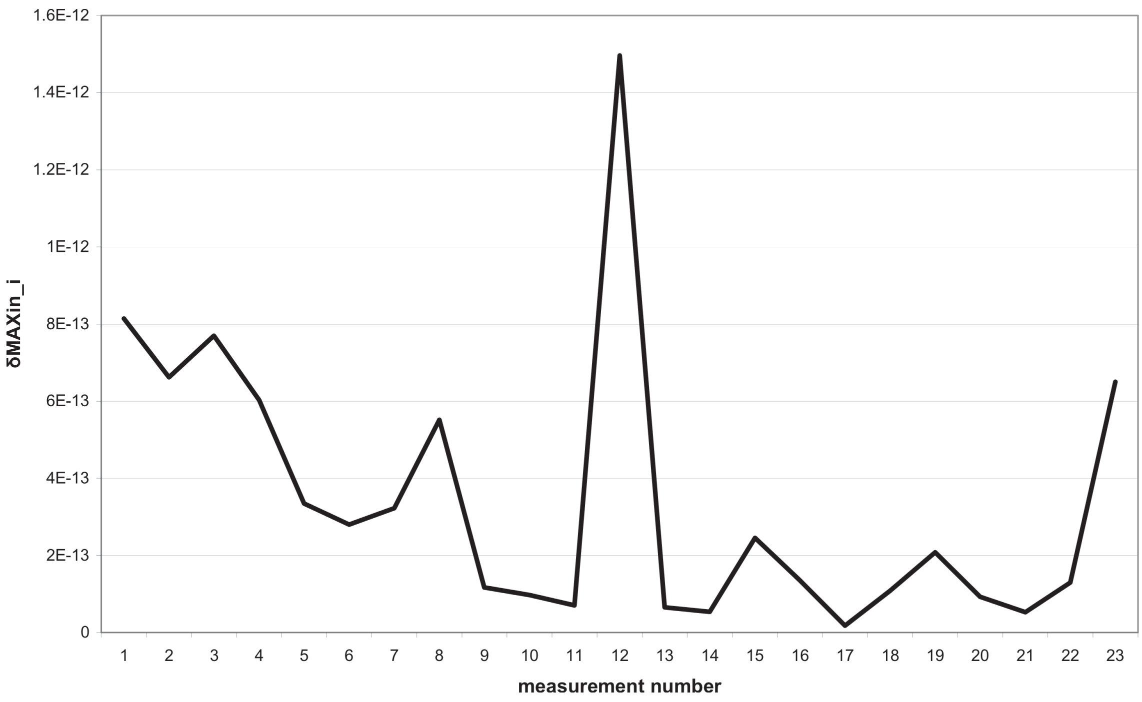

Fig. 9. Searched errors.

On the basis of [27] it was found that the error of the method in MRP increases with increasing of distance Sd and Sm. The method of determining the minimal value of error on outer and inner contour by using searching has become well-founded for this reason. On the basis of previous studies [27] the optimal values of N and NC were founded. For this reason, the article assumes it to be fixed. It was found that proposed random choice of independent variable (distance from the contour) is better than the sparse initial tabulation with possible zooming in the zone of expected extrema. On the basis of [27] it was concluded that for assumed measures of error for the internal contour it is not recommended to adopt fixed values for the solution to the internal contour.

In the first case, for given M, NC equal to 100 for problems I and II, and 120 for cases III-VII, Sd was searched in a range from 0.01 to 1 with step 0.01 for problems I-III and with step 0.005 for problems IV and V. In addition, Sm was searched in a range from 0.01 to E-0.01 with step 0.01 for problems I-III and 0.005 for problems IV and V – method I. This method turned out very time-consuming. A very large number of errors has to be searched for determining optimal values of the errors.

To reduce the number of searched points, value Sd was multiplied by random numbers generated from a range 0-1, M, NC remained constant/retained the same/constant value and the value of Sm was searched within the assumed range from 0.01 to E-0.01 for the cases I-III, and 0.005 for the cases IV-V – method II. In this way, in all studied cases, the amount of searched points was significantly reduced, what led to a reduction of 2,440 points in the most extreme case. The minimum values of errors on the outer and inner contour for cases I, III, IV and V are of the same range, as well as on the inner contour for the case II, as compared with searching within a given range of Sd. By contrast, for case II, the values of errors on the outer contour became deteriorated.

In the next step, the value of the Sm was multiplied by random value generated in a range 0–1, constant values M, NC were retained the same as in the previous methods and Sd was searched in a range from 0.01 to 1 with step 0.01 for cases I-III and 0.05 for IV and V – method III. By using random numbers, 800 points of search were assumed for cases I-III and 1580 for cases IV and V. As a result, the minimum values of errors on the internal contour for all studied cases and minimum values of errors on the outer contour for cases I, IV and V are comparable with the first of these methods, whereas minimum values of errors on the outer contour for cases II and III have deteriorated.

Also numerical experiments were carried out, which determined the Sd and Sm by multiplying established ranges of random values generated from the interval 0–1 and assuming values of M, NC from other methods – the method IV. In this case, only 100 values of errors were searched. Comparing with the first of these methods, for cases I, II and III, an increase of value of error occurred at the outer contour follows, while for cases II and V the same increase occurred on the internal contour. In other cases, the errors on the values of inner and outer contours were comparable.

Based on the numerical results presented in Tables 1–10, it can be concluded that the smallest values of error were obtained for case I and the largest for case III (square with square centered hole). The possible explanation of the large error in latter case can be the existence of the corners of the inner boundary. In the remaining cases when the inner contour or contours were smooth (circular) the values of error were much smaller.

The calculation of the dimensionless torsional stiffness was conducted for the circular with circular centered hole. The calculation of stiffness based on the approximate solution was completed by dividing of the cross section into triangular elements, which were integrated with the seven-point Gauss quadrature. The obtained results were compared with the exact formula for dimensionless stiffness of the annular region:

$$M_s = \frac{\pi}{2} \cdot \left(\left(\frac{1}{2} \right)^4 - E^4 \right). \tag{22}$$

Next, the result was compared with the results of the dimensionless stiffness resulting from Brendt's formula for the annular region:

$$M_{s-\text{Bredt}} = \frac{\pi}{4} \cdot \left(\frac{1}{2} + E \right)^3 \cdot \left(\frac{1}{2} - E \right). \tag{23}$$

The results of the comparison are presented in Fig. 10.

Table 1. The maximum value of the local error on an inner contour – the case I, $M = 100$, $NC = 100$, for optimum values of Sd and Sm.

E	Method I		Method II		Method III		Method IV	
	Inner contour	NES*	Inner contour	NES*	Inner contour	NES*	Inner contour	NES*
0.1	2.43E-15	360	3.47E-15	180	2.20E-15	800	8.13E-15	100
0.15	3.78E-15	520	4.64E-15	260	2.32E-15	800	5.32E-14	100
0.2	9.58E-14	760	1.37E-13	380	9.74E-14	800	1.52E-12	100
0.25	8.34E-12	960	1.00E-11	480	9.35E-12	800	5.27E-11	100
0.3	3.10E-10	1120	5.35E-10	560	3.79E-10	800	1.63E-09	100
0.35	9.32E-09	1320	1.29E-08	660	1.16E-08	800	3.81E-08	100
0.4	1.61E-07	1560	2.70E-07	780	1.64E-07	800	4.15E-07	100
0.45	3.98E-06	1760	5.98E-06	880	3.56E-06	800	7.35E-06	100

* NES – number of searched errors

Table 2. The maximum value of the local error on an outer contour – the case I, $M = 100$, $NC = 100$, for optimum values of Sd and Sm.

E	Method I		Method II		Method III		Method IV	
	Outer contour	NES*	Outer contour	NES*	Outer contour	NES*	Outer contour	NES*
0.1	7.76E-06	360	1.36E-05	180	2.65E-05	800	8.74E-03	100
0.15	8.18E-06	520	3.59E-05	260	1.22E-05	800	4.42E-04	100
0.2	8.46E-06	760	1.28E-05	380	1.00E-05	800	1.75E-04	100
0.25	9.38E-06	960	1.44E-05	480	9.93E-06	800	5.65E-05	100
0.3	1.15E-05	1120	1.68E-05	560	1.16E-05	800	3.76E-05	100
0.35	1.23E-05	1320	2.57E-05	660	1.46E-05	800	4.72E-05	100
0.4	2.07E-05	1560	2.99E-05	780	2.06E-05	800	4.22E-05	100
0.45	2.60E-05	1760	6.47E-05	880	3.80E-05	800	5.79E-05	100

Table 3. The maximum value of the local error on an inner contour – the case II, $M = 100$, $NC = 100$, for optimum values of Sd and Sm.

E	Method I		Method II		Method III		Method IV	
	Inner contour	NES*	Inner contour	NES*	Inner contour	NES*	Inner contour	NES*
0.1	1.29E-10	360	2.60E-10	180	1.60E-10	800	9.37E-06	100
0.15	1.70E-09	520	1.86E-09	260	1.97E-09	800	3.63E-05	100
0.2	1.46E-08	760	2.09E-08	380	1.84E-08	800	9.59E-05	100
0.25	1.49E-07	960	2.72E-07	480	1.68E-07	800	1.35E-04	100
0.3	1.73E-06	1120	2.71E-06	560	1.85E-06	800	5.45E-04	100
0.35	2.14E-05	1320	2.78E-05	660	2.12E-05	800	8.87E-04	100
0.4	2.61E-04	1560	3.41E-04	780	2.61E-04	800	4.55E-03	100
0.45	2.38E-03	1760	2.47E-03	880	2.59E-03	800	1.08E-02	100

Table 4. The maximum value of the local error on an outer contour – the case II, $M = 100$, $NC = 100$, for optimum values of Sd and Sm.

E	Method I		Method II		Method III		Method IV	
	Outer contour	NES*	Outer contour	NES*	Outer contour	NES*	Outer contour	NES*
0.1	1.08E-03	360	2.01E-01	180	2.20E-01	800	4.32E-01	100
0.15	1.03E-03	520	2.11E-01	260	1.17E-03	800	3.56E-02	100
0.2	1.21E-03	760	2.25E-01	380	1.60E-01	800	1.31E-01	100
0.25	9.24E-04	960	2.53E-01	480	1.75E-01	800	1.09E-02	100
0.3	1.08E-03	1120	1.96E-03	560	1.93E-03	800	3.24E-03	100
0.35	9.59E-04	1320	3.34E-01	660	2.31E-03	800	8.03E-03	100
0.4	1.17E-03	1560	3.05E-03	780	2.40E-03	800	1.45E-02	100
0.45	2.43E-03	1760	6.92E-01	880	7.40E-01	800	2.35E-01	100

Table 5. The maximum value of the local error on an inner contour – the case III, $M = 120$, $NC = 120$, for optimum values of Sd and Sm.

E	Method I		Method II		Method III		Method IV	
	Inner contour	NES*	Inner contour	NES*	Inner contour	NES*	Inner contour	NES*
0.1	6.17E-02	360	9.11E-01	180	2.09E-02	800	1.52E-02	100
0.15	9.30E-02	520	4.00E-01	260	6.28E-02	800	5.63E-02	100
0.2	2.54E-02	760	2.29E-01	380	2.77E-02	800	1.28E-02	100
0.25	1.56E-02	960	4.37E-02	480	3.74E-02	800	2.04E-02	100
0.3	5.93E-02	1120	1.14E-01	560	2.91E-02	800	9.14E-02	100
0.35	4.49E-02	1320	7.07E-02	660	3.96E-02	800	2.11E-02	100
0.4	1.52E-02	1560	1.66E-02	780	3.13E-02	800	9.20E-02	100
0.45	7.53E-02	1760	1.72E-02	880	1.32E-01	800	6.59E-02	100

Table 6. The maximum value of the local error on an outer contour – the case III, $M = 120$, $NC = 120$, for optimum values of Sd and Sm.

E	Method I		Method II		Method III		Method IV	
	Outer contour	NES*	Outer contour	NES*	Outer contour	NES*	Outer contour	NES*
0.1	1.30E-06	360	4.12E-06	180	1.22E-03	800	3.30E-04	100
0.15	1.40E-06	520	4.64E-06	260	6.48E-05	800	1.21E-03	100
0.2	1.68E-06	760	5.27E-06	380	5.37E-04	800	2.33E-03	100
0.25	1.75E-06	960	5.50E-06	480	4.59E-04	800	2.65E-03	100
0.3	1.94E-06	1120	6.16E-06	560	1.81E-03	800	3.15E-03	100
0.35	2.35E-06	1320	7.58E-06	660	9.06E-04	800	3.95E-03	100
0.4	3.13E-06	1560	1.07E-05	780	2.20E-03	800	5.40E-03	100
0.45	3.55E-06	1760	6.80E-02	880	3.12E-02	800	1.16E-02	100

Table 7. The maximum value of the local error on an inner contour – the case IV, $M = 120$, $NC = 120$, for optimum values of Sd and Sm.

E	Method I		Method II		Method III		Method IV	
	Inner contour	NES*	Inner contour	NES*	Inner contour	NES*	Inner contour	NES*
0.025	6.13E-09	160	6.15E-09	40	2.59E-04	1580	6.21E-09	100
0.05	7.68E-09	470	7.77E-09	120	3.33E-09	1580	9.02E-09	100
0.075	1.95E-09	940	4.89E-09	240	1.13E-09	1580	4.51E-09	100
0.1	1.44E-09	1340	3.89E-09	340	3.32E-09	1580	1.17E-08	100
0.125	1.54E-08	1740	1.64E-08	440	1.73E-08	1580	1.83E-08	100
0.15	6.12E-08	2040	6.65E-08	520	6.25E-08	1580	9.30E-08	100
0.175	3.94E-07	2440	4.07E-07	620	3.93E-07	1580	4.84E-07	100
0.2	1.20E-05	2920	1.22E-05	740	1.25E-05	1580	1.22E-05	100
0.225	2.57E-04	3320	2.58E-04	840	2.59E-04	1580	2.59E-04	100

Table 8. The maximum value of the local error on an outer contour – the case IV, $M = 120$, $NC = 120$, for optimum values of Sd and Sm.

E	Method I		Method II		Method III		Method IV	
	Outer contour	NES*	Outer contour	NES*	Outer contour	NES*	Outer contour	NES*
0.025	1.01E-05	160	8.09E-05	40	1.87E-02	1580	1.01E-05	100
0.05	1.06E-05	470	8.60E-05	120	1.69E-04	1580	1.11E-05	100
0.075	1.19E-05	940	6.34E-03	240	1.12E-03	1580	3.03E-05	100
0.1	1.43E-05	1340	3.55E-05	340	4.17E-04	1580	9.72E-05	100
0.125	1.95E-05	1740	6.32E-05	440	2.07E-05	1580	1.86E-04	100
0.15	3.27E-05	2040	5.08E-05	520	9.32E-05	1580	3.40E-04	100
0.175	8.46E-05	2440	2.96E-04	620	4.39E-04	1580	3.91E-04	100
0.2	3.96E-04	2920	2.09E-03	740	2.13E-03	1580	1.74E-03	100
0.225	4.21E-03	3320	1.05E-02	840	1.87E-02	1580	7.65E-03	100

Table 9. The maximum value of the local error on an inner contour – the case IV $M = 120$, $NC = 120$, for optimum values of Sd and Sm.

E	Method I		Method II		Method III		Method IV	
	Inner contour	NES*	Inner contour	NES*	Inner contour	NES*	Inner contour	NES*
0.025	4.02E-09	160	2.73E-09	40	6.21E-09	1580	2.33E-07	100
0.05	6.35E-09	475	5.20E-09	120	5.14E-09	1580	1.30E-08	100
0.075	7.56E-10	950	1.23E-09	240	1.97E-06	1580	1.49E-08	100
0.1	3.54E-09	1345	2.03E-09	340	3.10E-09	1580	2.42E-08	100
0.125	1.31E-08	1740	8.76E-09	440	1.69E-08	1580	4.78E-08	100
0.15	4.85E-09	1840	6.64E-08	520	7.82E-08	1580	1.14E-07	100
0.175	1.23E-06	2450	1.44E-06	620	1.97E-06	1580	1.46E-06	100
0.2	1.89E-05	2920	1.87E-05	740	1.97E-05	1580	1.94E-05	100
0.225	1.99E-04	3320	2.04E-04	840	2.00E-04	1580	2.10E-04	100

Table 10. The maximum value of the local error on an outer contour – the case IV $M = 120$, $NC = 120$, for optimum values of Sd and Sm.

E	Method I		Method II		Method III		Method IV	
	Outer contour	NES*	Outer contour	NES*	Outer contour	NES*	Outer contour	NES*
0.025	1.13E-03	160	3.16E-03	40	3.49E-03	1580	2.68E-03	100
0.05	1.15E-03	475	3.22E-03	120	7.91E-02	1580	2.89E-03	100
0.075	1.19E-03	950	7.15E-03	240	4.02E-01	1580	3.24E-03	100
0.1	1.25E-03	1345	2.80E-01	340	6.19E-03	1580	3.40E-03	100
0.125	1.33E-03	1740	3.45E-03	440	4.15E-03	1580	3.38E-03	100
0.15	1.25E-03	1840	3.30E-01	520	3.97E-03	1580	3.71E-03	100
0.175	1.52E-03	2450	1.64E-01	620	4.02E-01	1580	5.10E-03	100
0.2	1.83E-03	2920	4.68E-03	740	4.78E-03	1580	7.95E-03	100
0.225	2.79E-03	3320	5.57E-03	840	5.05E-03	1580	2.04E-02	100

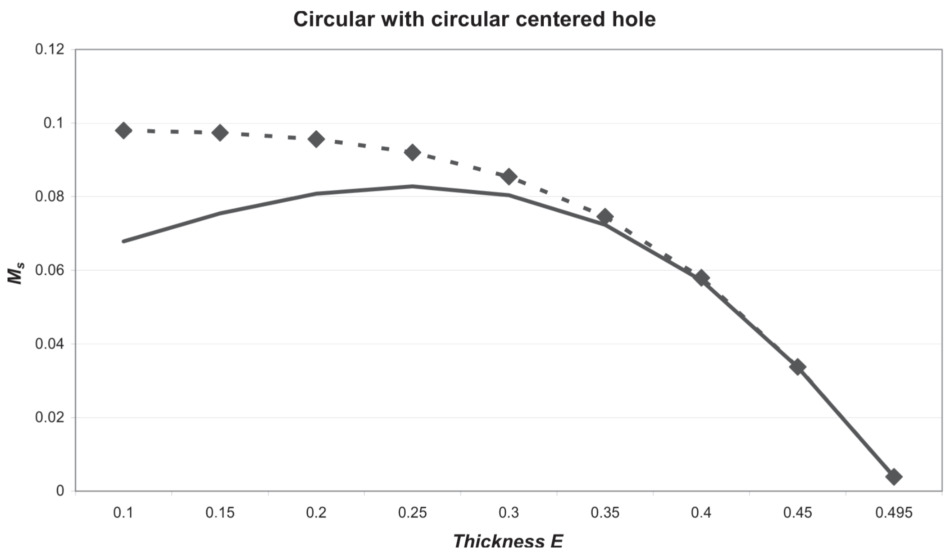

Fig. 10. Comparison of results given by proposed formula (19) – points, Bredt's formula (23) – solid line and exact solution (22) – broken line for circular with circular centered hole; $M = 46$, $NC = 46$.

7. Conclusion

The method of fundamental solutions was successfully applied to solve the boundary problem of the torsion of bars with multiply connected cross sections. On the basis of the numerical results for the circle with circular hole cross section of a bar, it was concluded that a well-known Brendt's method of calculating stiffness of thin-walled bars can be successfully applied to bars with the dimensionless thickness larger than $E = 0.4$. In all studied cases, it was observed that the boundary condition is satisfied. Stress function values along the X axis converge to zero, reaching zero at the edge of the outer section.

It was found that the introduction of random numbers particularly in searching of Sd significantly improved the speed of setting minimum value of errors. For the case of a circle with two symmetrically located round holes it was sufficient to search only 100 values of error to specify a minimum value. Application of random numbers, especially in case of a search of Sd, significantly increased the speed of finding the minimum error in comparison with other methods of searching.

References

[1] E. Weinel. The torsion problem for the eccentric annulus (in German). *Ingenieur Archivs*, **3**: 67–75, 1932.
[2] G. Polya, A. Weinstein. On the torsion rigidity of multiply connected cross-sections. *Annals of Mathematics*, **52**: 154–163, 1950.
[3] N.H. Arutyunyan, B.L. Abrahamian. *Torsion of elastic body* (in Rusian). *Gosudarstvennoe Izdatelstvo Fiziko-Matematicheskoj Literatury*, Moskwa, 1963.
[4] C.Y. Wang. Torsion of a flattened tube. *Meccanica*, **30**: 221–227, 1995.
[5] C.Y. Wang. Torsion of tubes of arbitrary shape. *International Journal Solids Structures*, **35**: 719–731, 1998.
[6] Y.Y. Kim, M.S. Yoon. A modified Fourier series method for the torsion analysis of bars with multiply connected cross sections. *International Journal Solids Structures*, **34**: 4327–4337, 1997.
[7] G. Mejak. Optimization of cross-section of hollow prismatic bars in torsion. *Communications in Numerical Methods in Engineering*, **16**: 687–695, 2000.
[8] J.A. Kołodziej, A. Fraska. Elastic torsion of bars possessing regular polygon in cross-section, *Computers & Structures*, **84**: 78–91, 2005.
[9] Z. Dyląg, A. Jakubowicz, Z. Orłoś. *Mechanics of materials* (in Polish), volume I. WNT, Warszawa, 1999.
[10] A. Morassi. Torsion of thin tubes with multicell cross-section. *Meccanica*, **34**: 115–132, 1999.
[11] G.R. Liu. *Mesh Free Methods. Moving beyond the Finite Element Method.* Boca Raton, CRC Press, 2003.
[12] M.R. Hematiyan, A. Doostfatemeh. Torsion of moderately thick hollow tubes with polygonal shapes. *Mechanics Research Communications*, **34**: 528–537, 2007.
[13] V.D. Kupradze, M.A. Aleksidze. The method of functional equations for the approximate solution of certain boundary value problems (in Rusian). *Zurnal Vycislennoj Matematiki i Matetyczeskoj Fizyki*, **4**: 683–715, 1964.
[14] R. Mathon, R.L. Johnston. The approximate solution of elliptic boundary value problems by fundamental solutions. *SIAM Journal on Numerical Analysis*, **14**: 638–650, 1977.
[15] A. Bogomolny. Fundamental solution method for elliptic boundary value problems. *SIAM Journal on Numerical Analysis*, **22**: 644–669, 1985.
[16] M. Katsurada. Asymptotic error analysis of the charge simulation method. *Journal of the Faculty of Science.* University of Tokyo, Section 1A, **37**: 635–657, 1990.
[17] M. Katsurada, H. Okamoto. A mathematical study of the charge simulation method. *Journal of the Faculty of Science.* University of Tokyo, Section 1A, **35**: 507–518, 1988.
[18] M. Katsurada, H. Okamoto. The collocation points of the fundamental solution method for the potential problem. *Computers & Mathematics with Applications*, **31**: 123–137, 1996.
[19] T. Kitagawa. Asymptotic stability of the fundamental solution method. *Journal of Computational and Applied Mathematics*, **38**: 263–69, 1991.
[20] T. Kitagawa. On the numerical stability of the method of fundamental solutions applied to the Dirichlet problem. *Japan Journal of Industrial and Applied Mathematics*, **35**: 507–518, 1988.
[21] G. Fairweather, A. Karageorghis. The method of fundamental solutions for elliptic boundary value problems. *Advances in Computational Mathematics*, **9**: 69–95, 1998.
[22] M.A. Golberg, C.S. Chen. The method of fundamental solutions for potential, Helmholtz and diffusion problems. In: M.A. Golberg, editor. *Boundary integral methods – numerical and mathematical aspects*, 103–176. Boston, Computational Mechanics Publications, 1998.
[23] K.H. Chen, J.H. Kao, J.T. Chen, D.L. Young, M.C. Lu. Regularized meshless method for multiply connected domain Laplace problems. *Engineering Analysis with Boundary Elements*, **30**: 882–896, 2006.
[24] Z-C. Li. The method of fundamental solutions for annular shaped domains. *Journal of Computational and Applied Mathematics*, **1**: 355–372, 2009.
[25] Th. Tsangaris, Y. S. Smyrilis, A. Karageorghis. Numerical analysis of the method of fundamental solutions for harmonic and biharmonic problems in annular domains. *Numerical Method for Partial Differential Equations*, **22**: 507–539, 2006.
[26] N.H. Arutyunyan, B.L. Abrahamian. *Torsion of prismatic rods* (in Rusian). Erevan, 1962.
[27] P. Gorzelanczyk, J.A. Kolodziej. Some remarks concerning the shape of the source contour with application of the method of fundamental solutions to elastic torsion of prismatic rods. *Engineering Analysis with Boundary Elements*, **24**: 633–641, 2007.